



Original Work

Role of Echogenic Amniotic Fluid Particles and Optical Density in prediction of Respiratory Distress Syndrome and Labor

Dr. Shankar H S Ram ^{*Ψ} MBBS and Dr. Sandhya Ram* DA

*Research Assistant, Sandhya Ram Maternity Hospital, Palghat, Kerala, India

(Received 18 March 2009 and accepted 31 May 2009)

ABSTRACT: This study was aimed to correlate echogenic amniotic fluid particle size (AFPS) in late third trimester to fetal lung maturity and amniotic fluid optical density (AFOD) at labor. AFPS were measured with specified criteria by real time transabdominal USG (3.5MHz) while Amniotic Fluid Index (AFI) was measured during routine antenatal visits. The criteria for AFPS score which are taken into account are the amniotic fluid particle size, number and distribution. Serial AFPS measurements were done till onset of labor. AFPS was correlated to AFOD value at spontaneous labor in 123 women. Uncentrifuged fresh amniotic fluid samples were obtained during ARM/amniotomy and used for AFOD estimation at 650 nm. The mean AFPS and AFOD at onset of labor was found to be 5.14 ± 0.69 mm ($3.67 - 6.7$ CI 95%) and 1.03 ± 0.31 (0.35 -1.69 CI 95%) respectively in 116 women who delivered normal babies devoid of respiratory distress syndrome (RDS). Serial AFPS measurements showed a definite AFOD surge after a value in the region of 3.8 mm which is obtained culminating in onset of Labor. 28 women (24.1%) had dense clusters of free floating particles across the vertical pool in amniotic fluid with mean AFPS and AFOD of 5.6 ± 0.68 mm and 1.12 ± 0.21 respectively. In 123 women, AFPS < 3.8 mm had sensitivity of 85.74% and positive predictive value of 66.67% in predicting RDS. AFPS serves as a sonological marker for fetal lung maturity and labor. The range of AFOD values can be measured in terms of AFPS ($r = 0.6$, $F = 69.8$, $\beta = + 0.23$, $p < 0.001$). Serial AFPS estimation predicts fetal maturity and onset of labor.

KEY WORDS: Amniotic fluid; Particle size; Optical density; Respiratory distress syndrome; Labor

INTRODUCTION

Many authors attempted to explore the various fetomaternal interactions and associated changes in the amniotic fluid and maternal serum in women who were in preterm, term and near labor. Cetrulo et al¹ have correlated amniotic fluid turbidity assayed by OD at 650 nm and the respiratory surfactants in amniotic fluid. There is a surge in sebaceous gland activity, size and number, producing sebum, which is primary constituent of vernix caseosa, before the onset of term labor. The lung skin

interactions by the surfactant causes the induction of vernix detachment from the fetal skin surface which is the primary factor leading to increase in amniotic fluid turbidity as the lung matures². The rapidly raising surfactant levels in amniotic fluid may be responsible for the surge in the AFOD near the onset of spontaneous labor.

Levels of pro labor cytokines like IL-6, IL-8, IL-1 beta and EGF in amniotic fluid and maternal serum that are elevated during progress of labor, are produced by the human amniotic fluid cells³⁻⁶. Cytokines like IL-1 which is highly expressed by corneocytes, is present in the normal human sebaceous gland and serves as a signal for onset of parturition⁷⁻⁹. IL-1 beta increases the production of matrix metallo protease (MMP)-1, 3 and 9. IL-1, 2, 3 and 6 can stimulate the prostaglandin

^ΨCorrespondence at: Mobile No. +919447737206, 919447737207; Email: ram.hss83@gmail.com

biosynthesis by intrauterine tissues. Cytokines also induce hyaluronic acid production by cervical fibroblasts, which may promote cervical ripening. Spontaneous rupture of membranes at term or preterm and microbial invasion, show increased expression of MMP 8 and 9. Preterm labor could be non infectious and an uncomplicated aseptic inflammatory process¹⁰⁻¹³. Placental maturity (placental clock) and corticotropin releasing hormone do play a role in cytokine and prostaglandin pathways¹⁴. The AFOD changes reflect the processes that precede the more rapid and dramatic events of parturition.

The mature levels of pulmonary surfactant are usually present after 35 weeks of gestation¹⁵. The levels of surfactant protein A, IL-1 beta are increased in amniotic fluid during labor¹⁶. Also there is an increase in the lamellar body count towards the end of gestation¹⁷. Amniotic fluid particles are the major contribution to optical density. Previous studies of fetal lung maturity vary from ability to read news prints across test tubes containing amniotic fluid to quantitative LS ratio estimation¹⁸.

The source of the particles may differ trimester by trimester¹⁹. Free floating particles (FFPs) have been correlated to congenital malformations likely to bleed and anencephaly in second trimester²⁰⁻²¹. Sonological studies have shown that amniotic fluid particles in third trimester are nothing but vernix (100% sensitivity) and less likely due to meconium, and the possibility of meconium stained liquor cannot be ruled out fully²²⁻²³. FFPs exhibiting snow storm and blizzard appearance in amniotic fluid can be used to evaluate fetal lung maturity by realtime ultrasound²⁴. Earlier Parulekar et al²⁵ had studied the amniotic fluid particles considering the size of largest echogenic amniotic fluid particle at different gestational age.

The purpose of this study is to demonstrate the changes in AFOD through gestation and as a marker for onset of labor in terms of AF particles. The correlation of AFPS and AFOD pertaining to onset of labor and fetal maturity is attempted with specified criteria in this study. Size of the particles remains a measurable parameter and serves as an index of optical density and hence the physiological processes that contribute to the onset of labor.

METHODOLOGY

Study sample

The study was conducted in 123 pregnant women of age group ranging from 19 years to 37 years with a singleton gestation. They

attended the department of Obstetrics, Sandhya Ram Maternity Hospital, Palghat, Kerala with reliable dates of LMP and delivered after spontaneous onset of labor. Crown rump length estimation was used for dating. A complete case record form of every patient was maintained including a detailed history, clinical examination, USG findings, obstetric examination and the results of all investigations recorded at each visit. None of the women were taking any medication in the past and all patients underwent routine laboratory screening. Demographic variables of each patient such as age, gravidity, parity, reproductive history, race, blood transfusion history, birth weight, 1 and 5-minute APGAR and Bishop Scores were recorded. The database made out of our hospital case records was analyzed retrospectively. This study conforms to standards set by the declaration of Helsinki.

Exclusion criteria: Amniotic fluid samples obtained from women with following criteria are excluded from this study:

- Any medical maternal high risk factor (e.g. Diabetes mellitus, Gestational diabetes mellitus, Chronic hypertension, Pregnancy induced hypertension, Rheumatic heart disease, other endocrine disturbances, renal disease)
- History of receiving steroid therapy
- Intra-uterine growth retardation or macrosomic fetuses
- No obstetric ultrasonography for gestational age dating available
- Ante partum hemorrhage
- Presence of meconium stained amniotic fluid
- Fetal malformations
- Multiple pregnancies
- Elevated WBC counts
- Premature Rupture of Membranes
- AFI less than 9
- AFI more than 16
- Measurements taken within 12 hrs before active labor

Technique

Amniotic fluid sample collection at amniotomy in laboring patients: The membranes were visualized per Sims speculum examination with good source of light. A 23 G spinal needle fitted with 2 ml disposable syringe was used to pierce the membrane and draw the amniotic fluid sample. Membranes were pierced while uterus was not acting and membranes were not under tension.

Method of measurement of echogenic amniotic fluid particles: The echogenic amniotic fluid particles were measured in all the women at first stage of labor (intact membranes), prior to artificial rupture of membrane (ARM) / active phase and enhanced uterine contractions, with 3.5 MHz transabdominal real time ultrasonography. Serial measurements were taken on routine antenatal visits.

Appearance of echogenic AFPs vary from on and off minute dots, scantily scattered or sparsely distributed particles to uniform flakes, swarm of bees' appearance and densely packed clusters of particles of varying sizes. It includes scale like picture, mosaic pattern, exhibiting Brownian or swirling movement near the limb buds, snowstorm and blizzard appearance in one to all the AF pockets in 4 quadrants with advancing gestational age. Free echogenic AFPs in late third trimester exhibiting independent motion that tend to settle down and having well defined margins are considered for estimation of the size along its longest distinct linear dimensions. After screening all the quadrants for amniotic fluid particles, the size of particles are measured in millimetre (mm) from the multiple frozen magnified USG frames initially in two of the quadrants preferably with maximum number and distribution of particles. The measurements are arranged in descending order. The average size of first and second largest particle is taken as the echogenic AFPS for that quadrant. If the difference between size of first and second particle is more than 0.5 mm, the average of three largest particles should be considered in estimation of echogenic AFPS of that quadrant. If at all the difference between the first and second largest particle is more than 1.5 mm the first largest particle is excluded.

Likewise, the measurements are taken for other quadrants. If the echogenic AFPS of either of the two quadrants is less than 4.8 mm, the measurements should be taken in 3 quadrants. A final average out of the 3 or 2 quadrants is taken as echogenic AFPS. AFPs appearing very small (< 1.5mm) or not seen in well defined AF pocket are taken as zero mm. If snowstorm or blizzard appearance for the entire depth of AF pocket is noted in any of the quadrants, a value of 1 mm is added to the estimated AFPS.

To simplify and summarise, at least 2-3 large particles in similar range are measured in each

of 2-3 quadrants at optimal AFI. A final average of size of particles sampled in clusters is taken as AFPS. **Figure 1** shows well defined echogenic AFPs with varying size, number and distribution (sparse, dense, and very dense/snowstorm) in USG images which are arranged to corresponding range of AFOD values obtained during our study. Bottom of the figure demonstrates the naked eye appearance of Amniotic fluid arranged with increasing AFOD.

Statistics

Statistical analysis was done using SPSS 15.0. The graphs were drawn using Microsoft excel and Adobe Photoshop 6. P value of < 0.05 is considered significant.

RESULTS

The Mean AFOD and echogenic AFPS in all pregnancies at onset of labor was found to be 0.99 and 4.9 mm respectively. The Details of AFOD, AFPS and RDS at different gestational age groups are summarised in **Table 1**. The values of AFOD at 650nm of uncentrifuged fresh amniotic fluid samples were obtained and plotted against the echogenic AFPS at onset of labor (**Figure 2**). **Figure 3** shows exponential trend of serial AFPS measurements (minimum 3 values were taken for plotting) in 101 women as represented by each of the lines. The final values on the series were taken at first stage of labor to demonstrate definite surge. A progressive increase in size, number and distribution (sparse to dense) was noted and measured in all cases in terms of AFPS score.

Figure 4 shows serial measurements of echogenic amniotic fluid particle size (AFPS) in millimetres (mm) when plotted against gestational age (days) in 17 women among 123. The figure represents the finer short term variations of surge in detail point to point of values. It is a magnification and fine adjustment of **figure 3**. There is a slow and prolonged rise in AFPS in third trimester as gestational age advances followed by an exponential rise with varying slopes culminating in the onset of labor. The end point denotes onset of labor. The rapid rise in AFPS denotes a corresponding AFOD surge. One of the women had a zigzag pattern. **Figure 5** represents AFPS at different Gestational age (days) when the women were in labor.

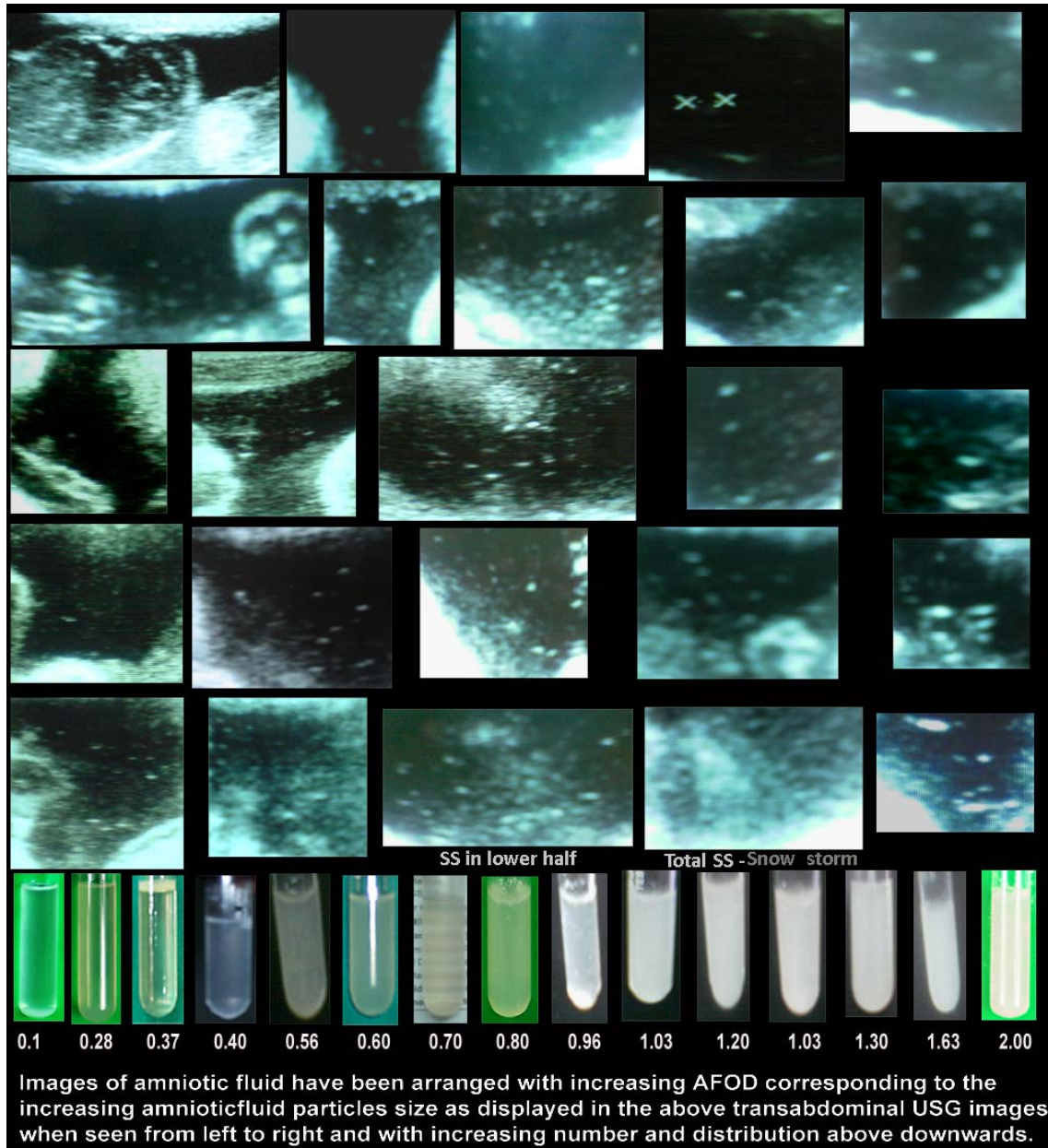


Figure 1: Showing echogenic AFPs in USG images and naked eye appearance of amniotic fluid

Table 1: Descriptive analysis of AFOD, AFPS, snowstorm appearance and RDS

Factor(Mean±SD)	< 259 days Group 1	259–270 days Group 2	>270-days Group 3	Total	RDS (-)	RDS (+)	SS (+)
AFOD AT LABOR	0.50±0.52	0.93±0.35	1.08±0.29	0.99±0.35	1.03±0.31	0.19±0.07	1.12±0.21
AFPS AT LABOR	2.7 ±1.6	5.0 ± 0.78	5.1±0.67	4.9±0.95	5.14±0.69	2.4±1.09	5.6±0.68
SS (+) n	1	12	15	28	28	0	28
RDS (+) n	5	2	0	7	0	7	0
Samples size (n)	7	50	66	123	116	7	28

Placenta Grade (Mode-Grade II). GA (Mean±SD) = 270.7±8.2 days. (n=123).
 SS- Snow storm/Dense AFPs Clusters in full depth of VP (at least in 1 vertical pool of Amniotic fluid)
 Difference in AFOD and AFPS b/w Groups 1-2, 1-3 p < 0.05 & 2-3 p > 0.05 (t test).

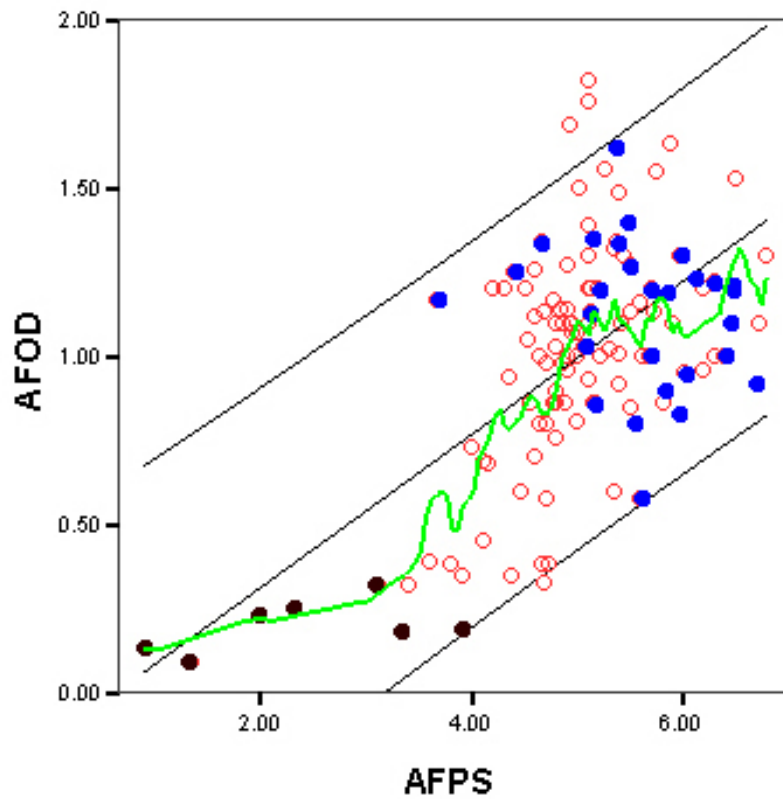


Figure 2: AFOD at 650 nm is plotted against echogenic AFPS in mm (n=123. $r=0.6$, $F = 69.8$, $\beta = + 0.23$, $p < 0.001$). The smooth green line passes through the values of AFOD corresponding to the AFPS between 95% individual prediction interval lines of linear regression model. AFPS < 3.8mm Vs RDS (\pm) has sensitivity = 85.74% and PPV = 66.67%. A value of AFOD of 0.99 which is the mean AFOD at onset of labor, corresponds to AFPS of around 5 mm. The black dots represent cases of RDS (n=7) with AFOD value < 0.35. Blue dots represent cases who had snow storm appearance (n=28).

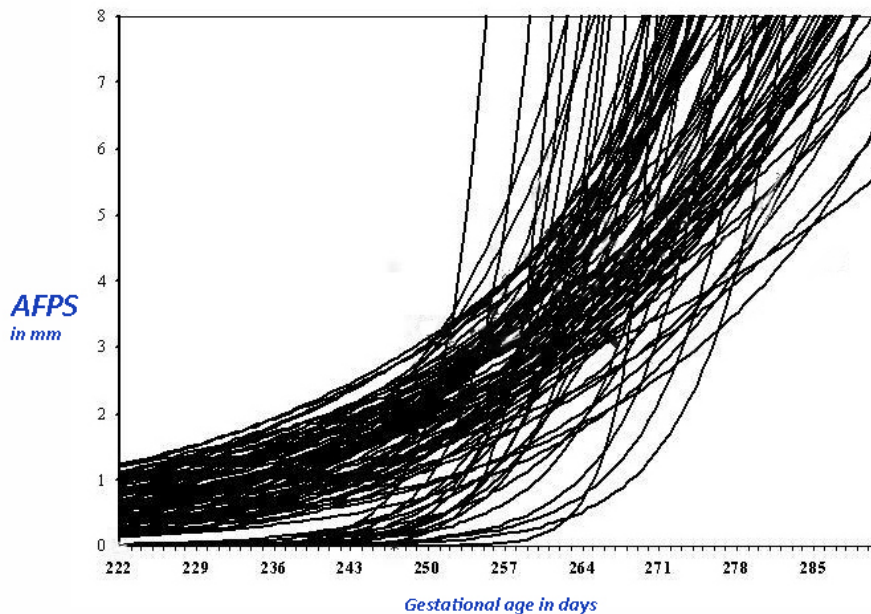


Figure 3: Exponential trend of AFPS measurements

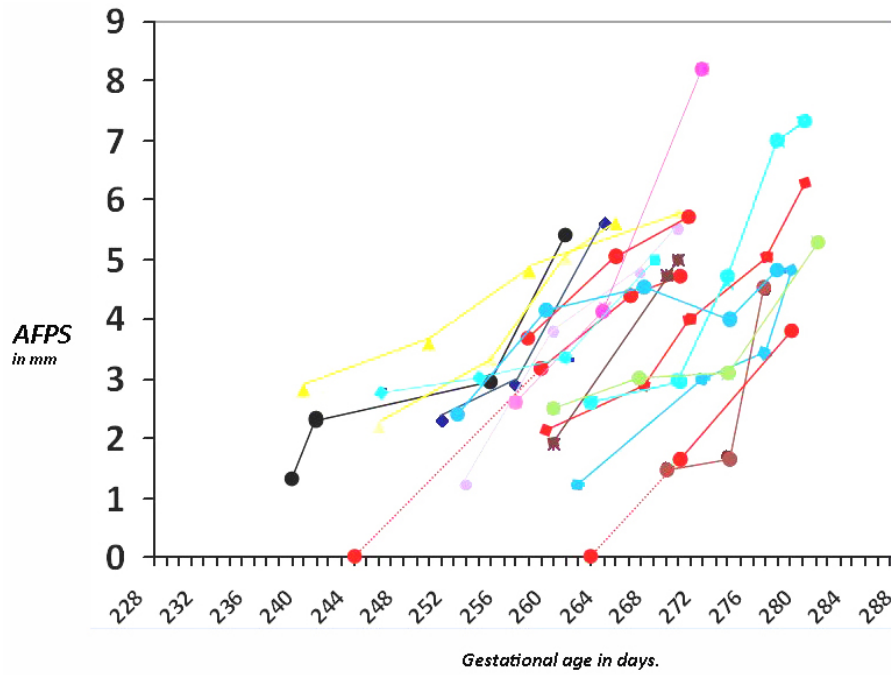


Figure 4: Echogenic amniotic fluid particle size (AFPS) as per gestational age

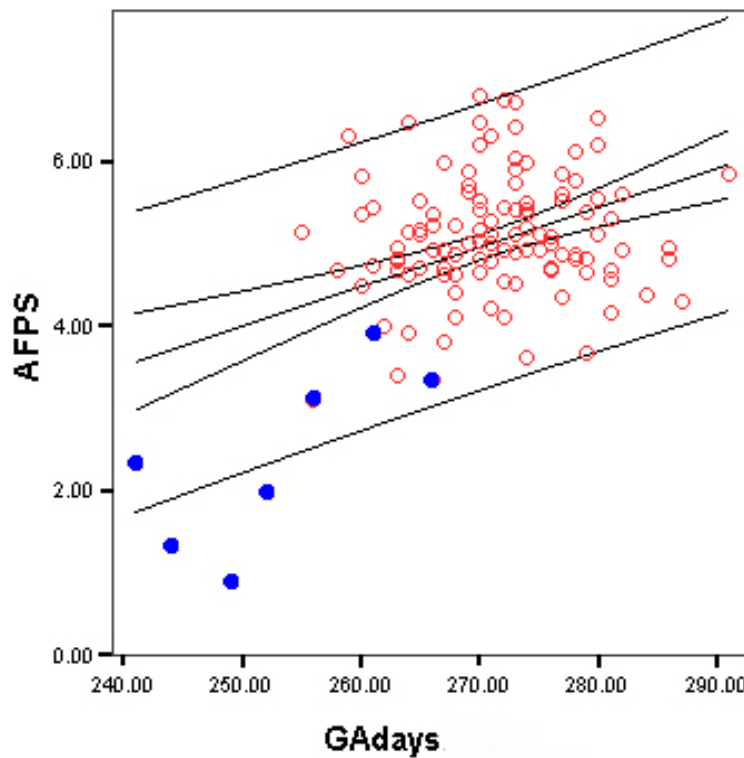


Figure 5: AFPS at labor; blue dots represent cases of RDS

DISCUSSION

We hypothesise that AFOD is definite marker for labor as well as fetal lung maturity. The findings of our study shows that the

corresponding range of AFOD can be measured indirectly using AFPS avoiding amniocentesis. The AFPs begin to appear at 35 to 36 weeks of gestation. Initially, they are few in number, smaller in size (2mm), freely

mobile and appear in one or two quadrants. The number, size and distribution of the particles increase gradually and extend to other quadrants. The changes are more dramatic in 1-2 weeks prior to onset of labor. This rapid increase in the size of the particles, and its number and density tend to appear more towards the end of gestation.

The mean AFOD and AFPS at onset of labor was found to be 1.03 ± 0.31 (0.35 - 1.69 CI 95%) and 5.14 ± 0.69 mm (3.67 - 6.7 CI 95%) respectively in 116 women who delivered normal babies. Seven out of 123 women had delivered babies with varying degrees of RDS having mean AFOD and AFPS as 0.19 ± 0.07 and 2.4 ± 1.09 mm respectively. RDS was severe at gestational age below 37 weeks. A definite surge in AFPS could not be demonstrated in them. The mean AFPS was found to be nearly half of that of women who delivered normal babies.

The snowstorm appearance, blizzard patterns and dense clusters of AFPs are seen usually at a higher AFOD values (> 0.80) and more appreciated with fetal movements on ultrasonography. In our study, the snow storm appearance in at least one vertical pool for the entire depth was noted in 22.7% women under who did not develop RDS. The mean AFOD was 1.12 ± 0.21 (4.4 - 6.7 95% CI) and AFPS were 5.6 ± 0.68 mm (0.80 - 1.40 95%CI) respectively.

Based on the results of our study we observed that an AFOD value of < 0.40 and AFPS < 4 mm at labor increases the risk for RDS of varying degrees. 17 women (**Figure 4**) who delivered babies without RDS had slow and prolonged rise of AFPS till about 3.8 mm corresponding to AFOD in the region of 0.40 (**figure 2**), followed by surge in AFPS culminating in labor. The graph exhibiting giraffe pattern (**figure 4**) is similar to serum hyaluronic acid levels during pregnancy and labor associated with cervical ripening culminating in parturition as shown by Kobayashi et al²⁶.

There is a large variability in the duration (1 to 2 weeks, occasionally few days)²⁷ and slope of the surge during which the AFPS is ranged from 3.5 to 4.5 mm prior to onset of labor (**figure 4 and 2**). Within this range, 18 women (AFOD ranged from 0.19 to 1.25) delivered having AFOD ranged from 0.19 to 1.25. Amongst these, 4 women had AFOD < 0.40 . One out of 18 women delivered a baby who developed RDS. Hence, the precaution with intervention should be taken in these cases. None of the babies had RDS with AFPS > 4.5 mm in our study despite of having 2 women (Out of 101) of AFOD < 0.40 (0.33 and 0.38).

An AFPS of 5.1 mm which is the mean AFPS of 116 women at onset of labor who delivered normal babies, corresponds to AFOD in the region of 1.00 (**figure 2**). Therefore, we infer that the AFOD surge begins at AFOD around 0.40 and terminate in labor at an optimum AFOD around 1.0.

Our results confirm the hypothesis that lung maturity progresses with the AFOD surge culminating in onset of normal labor. Thus, preparations for labor start at about 8 to 12 days prior to the onset of spontaneous labor as indicated by AFOD surge and its duration. The Serial USG evaluation of AFPS shall predict fetal lung maturity and labor. The variations and exceptions to AFOD surge has to be explored with a multifactorial background (age, BMI and mutations of oxytocin receptors) along with other coexisting obstetric and sonological parameters. There could also be several alternate pathways in normal labor²⁸

It is apparent that an increase in AFOD levels occurs in parallel to sequence of events culminating in parturition. Further studies are needed to correlate the levels of serum and AF markers with AFOD to explain the physiology of onset and progression of labor. We postulate that AFOD which can be measured and expressed in terms of AFPS values, is a definite sonological marker for lung maturity and labor and also helpful in predicting the onset of labor after serial AFPS measurements (definite surge as noted by at least two serial values after 36 weeks with doubling AFPS values over 1-2 weeks exceeding 4.5 mm near mean gestational age) that enables prior admission and institutional monitoring of all stages of labor. It also guides to deal with women in third trimester who did not have a reliable menstrual history or dating scan and as a step prior to confirming fetal maturity by amniocentesis when conditions arise.

Limitation of study

Inter and intra operator and USG variations under various resolutions needs metaanalysis. The AFPS may not be the exact measurements of actual amniotic fluid particle dimensions. There is a definite possibility of missing meconium stained liquor which is significant in view of neonatal outcome. The echogenicity of the fluid content apart from the AF particles may alter the contrast. The appearance, homogeneity of distribution, AFPS and number of AFPs vary with progress of labor/enhanced uterine contractions though not in all women. This requires serial measurements of AFPS and its documentation. The Degeneracy of AFPS in determining

AFOD makes the association only an approximation and not an equivalent to gold standard (AFOD). Last but not the least, the ability of the fetus to produce vernix itself may exhibit polymorphism.

CONCLUSION

Fetal lung maturity is followed by AFOD surge culminating in the onset of labor. AFOD which can be measured serially in terms of AFPS serves as a marker for labor and also predicts RDS. This basic knowledge about AFOD and simple cost effective noninvasive methodology can be used for programming and optimising labor, and improve perinatal outcome. This study can be a basis of many other studies that can help in understanding the process of initiation of labor and its dysfunction better and open up new avenues for labor induction and monitoring in the times to follow. It is possible now to initiate safe labor that simulates a spontaneous labor and plan an elective LSCS with predictable perinatal outcome as guided by AFPS as an obstetric parameter.

REFERENCES

1. Cetrulo CL, Sbarra AJ, Selvaraj RJ, et al. Positive correlation between mature amniotic fluid optical density reading and the absence of neonatal hyaline membrane disease. *J Reprod Med.* 1985 Dec;30(12):929-32.
2. Narendran V, Wickett RR, Pickens William L, et al. Interaction between pulmonary surfactant and vernix: a potential mechanism for induction of amniotic fluid turbidity. *J Pediatric Research.* 2000 Jul;48(1):120-4.
3. Mazzucchelli I, Avanzini MA, Ciardelli L, et al. Human amniotic fluid cells are able to produce IL-6 and IL-8. *Am J Reprod Immunol.* 2004 Mar;51(3):198-203.
4. Gundula H, Alfred AG, Peruka et al. The relationship between cervical dilatation, Interleukin 6 and Interleukin-8 during term labor. *Acta Obstet Gynecol Scand.* 2001 Sep;80(9):840-8.
5. Romero R, Wu YK, Oyarzun E, et al. A potential role for epidermal growth factor/alpha-transforming growth factor in human parturition. *Eur J Obstet Gynecol Reprod Bio.* 1989 Oct;33(1):55-60.
6. Annells MF, Hart PH, Mullighan CG, et al. Interleukins-1, -4, -6, -10, tumor necrosis factor, transforming growth factor-beta, FAS, and mannose-binding protein C gene polymorphisms in Australian women: Risk of preterm birth. *Am J Obstet Gynecol.* 2004 Dec;191(6):2056-67.
7. Romero R, Parvizi ST, Oyarzun E et al. Amniotic fluid interleukin-1 in spontaneous labor at term. *J Reprod Med* 1990 Mar;35(3):235-8.
8. Anttila HS, Reitamo S, Saurat JH. Interleukin 1 immunoreactivity in sebaceous glands. *Br J Dermatol.* 1992 Dec;127(6):585-8.
9. Burkhart CN. Clinical assessment of acne pathogenesis with treatment implications. *Int Pediatr.* 2003;18(1):14-9.
10. Pankaj D. Cytokines in Obstetrics and Gynecology. *J Obstet Gynecol India.* 2007;57(3):205-9.
11. Locksmith GJ, Clark P, Duff P, et al. Amniotic fluid concentrations of matrix metalloproteinase 9 and tissue inhibitor of metalloproteinase 1 during pregnancy and labor. *Am J Obstet Gynecol.* 2001 Jan;184(2):159-64.
12. Biggio JR Jr, Ramsey PS, Cliver SP, et al. Midtrimester amniotic fluid matrix metalloproteinase-8 (MMP-8) levels above the 90th percentile are a marker for subsequent preterm premature rupture of membranes. *Am J Obstet Gynecol.* 2005 Jan;192(1):109-13.
13. Challis JR, Sloboda dm, Alfaidy N, et al. Prostaglandins and mechanisms of preterm birth. *Reproduction* 2002 Jul;124(1):1-17.
14. Wadhwa PD, Porto M, Garite TJ, et al. Maternal corticotropin-releasing hormone levels in the early third trimester predict length of gestation in human pregnancy. *Am J Obstet Gynecol.* 1998 Oct; 179(4):1079-85.
15. Respiratory tract Disorders: Hyaline membrane Disease. In: Richard E Behrman, Hal B Jenson, Robert Kliegman. *Nelson text Book of Pediatrics.* 16th ed. 2000:499.
16. Parturition & Surfactant Protein A. Cytokine Bulletin, R&D systems 2004 retrieved from http://www.rndsystems.com/cb_detail_objectname_SU04_ParturitionSurfactantProteinA.aspx.
17. Khazardoost S, Yahyazadeh H, Borna S, et al. Amniotic fluid lamellar body count and its sensitivity and specificity in evaluating of fetal lung maturity. *J Obstet Gynecol.* 2005 Apr;25(3):257-9.
18. Strong TH Jr, Hayes AS, Sawyer AT, et al. Amniotic fluid turbidity: a useful adjunct for assessing fetal pulmonary

- maturity status. *Int J Gynaecol Obstet.* 1992 Jun;38(2):97-100.
19. Hallak M, Zador IE, Garcia EM, et al. Ultrasound-detected free-floating particles in amniotic fluid: correlation with maternal serum alpha-fetoprotein. *Fetal Diagn Ther.* 1993 Nov-Dec;8(6):402-6.
 20. Vengalil S, Santolaya-Forgas J, Meyer W, et al. Ultrasonically dense amniotic fluid in early pregnancy in asymptomatic women without vaginal bleeding: A report of two cases. *J Reprod Med.* 1998 May;43(5):462-4.
 21. Cafici D, Sepulveda W. First-trimester echogenic amniotic fluid in the acrania-encephaly sequence. *J Ultrasound Med.* 2003 Oct;22(10):1075-9.
 22. Brown DL, Polger M, Clark PK, et al. Very echogenic amniotic fluid: ultrasonography-amniocentesis correlation. *J Ultrasound Med.* 1994 Feb;13(2):95-7.
 23. David MS, Jacques SA, Susan AS, et al. Sonographically homogeneous echogenic amniotic fluid in detecting meconium-stained amniotic fluid. *Obstet Gynecol.* 1991 Nov;78(5 Pt 1):819-22.
 24. Gross TL, Wolfson RN, Kuhnert PM, et al. Sonographically detected free-floating particles in amniotic fluid predict a mature lecithin-sphingomyelin ratio. *J Clin Ultrasound.* 1985 Jul-Aug;13(6):405-9.
 25. Parulekar SG. Ultrasonographic demonstration of floating particles in amniotic fluid. *J Ultrasound Med.* 1983 Mar;2(3):107-10.
 26. Kobayashi H, Sun GW, Tanaka Y, et al. Serum hyaluronic acid levels during pregnancy and labor. *Obstet Gynecol.* 1999 Apr;93(4):480-4.
 27. Ram S, Sandhya, Ram S, et al. Amniotic fluid particles and optical density at term - a case report. *The Internet Journal of Gynecology and Obstetrics.* 2009;11(1): http://www.ispub.com/journal/the_internet_journal_of_gynecology_and_obstetrics/volume_11_number_1_6/article_printable/amniotic_fluid_particles_and_optical_density_at_term_a_case_report.html
 28. Susanne AT. Mediators of cervical ripening in preterm birth: experimental and clinical investigations. Thesis from department of women and child health division of obstetrics and gynecology, Karolinska Institute, Stockholm; Sweden 2005. Retrieved from <http://diss.kib.ki.se/2005/91-7140-305-1/>